Orientation Behavior of Retinal Photoreceptors in Alternating Electric Fields

M. Radu,*† M. Ionescu,*‡ N. Irimescu,§ K. Iliescu,* R. Pologea-Moraru,* and E. Kovacs*

*Biophysics and Cellular Biotechnology Department, Carol Davila University of Medicine and Pharmacy, Bucharest, Romania; †Horia Hulubei National Institute for Physics and Nuclear Engineering, Bucharest, Magurele, Romania; ‡Diabetes and Nutrition Department, N. Malaxa Hospital, Bucharest, Romania; and §National Institute of Infectious Disease, "Prof. Dr. Matei Bals", Bucharest, Romania

ABSTRACT In alternating electric (AC) fields, particles experience polarizing effects that induce dipoles that orient elongated specimens either parallel or perpendicular to the field lines. In this work we studied the behavior of photoreceptor cells' rod outer segments (ROS) in AC fields of different frequencies. We showed that at low frequencies, ROS orient parallel to the field, whereas at higher frequencies they orient perpendicular to the field lines (in the frequency range from 100 Hz to 10 MHz). We found this behavior to be dependent on the physiological state of cells (due to modifications in their electrical properties). To simulate cell damage, the membrane conductivity was changed by treating the cell with gramicidin A, which resulted in a decrease of cytosol conductivity and, consequently, in a change of the orientation behavior of the treated cells. The change of cell orientation with cytosol conductivity is rather sharp, suggesting the potential of the method for accurate evaluation of the cell physiological status. We modeled the interaction between ROS and AC fields approximating the rod cell by a prolate spheroid with a very long axis. The internal compartment of the ellipsoid was considered to be filled with an inhomogeneous medium consisting of alternating layers of membrane and cytoplasm as media modeling the disks. This theoretical model proved to be in good agreement with the experimental results and enabled the derivation (by fitting with the experimental results) of the membrane and cytosol parameters for normal and damaged cells.

INTRODUCTION

Living cells in suspension may respond to an alternating (AC) field by orienting, deforming, moving, or rotating. These effects originate in the interfacial polarization produced by AC field at the structural interfaces within the cell. Interaction of the induced cellular dipole with the external field results in translation or rotation of cells, according to their dielectric properties (1–4).

Some of the experimental methods based on the described effects are electrokinetic techniques: dielectrophoresis (5–8), electroorientation (9–16), electrorotation (6,17,18), and traveling wave devices (6). These techniques are essentially used for manipulating and separating cells based on their electrical properties as well as for cell characterization (1). Haibo and Bashir succeeded in separating living and dead bacteria in a mixture using dielectrophoresis (19). Electrorotation was used to characterize different types of cell lines; i.e., lymphocytes fractions (20) and yeasts (16). It was suggested that dielectrophoresis is more sensitive than standard methods (DNA fragmentation assay and annexinV assay) for detecting apoptotic cells (21).

Electroorientation is the frequency-dependent orientation of elongated particles in AC fields. The stable position of the cell in the field is determined by the torque resulting from interaction between the field and the polarized cell. Depending on frequency of the applied field, dipoles induced in elongated cells determine their orientation either parallel or perpendicular to the field lines (12). The phenomenon was evidenced for several types of elongated cells, such as yeast (most commonly *Schizosaccharomyces pombe* (5,8,9,14, 22)), erythrocytes (12), bacteria (16), and algae (12). As predicted by theoretical models, the frequency at which the cells change their orientation with respect to the field direction—the so-called turnover frequency (10)—depends on the electrical and geometrical parameters of the cells and on the conductivity of the suspension medium (9,10, 13–15). Consequently, the electroorientation spectrum—defined as the dependence of the turnover frequency on the external electric conductivity—divides the diagram in two or three distinct areas, one for each possible cell orientation (12,13).

Photoreceptor rods are very special elongated cells. As part of the retina, the rod outer segments (ROS) are physically anchored in the eye nerve. The internal structure of the rods is complex, hundreds of membrane sacs (disks) being packed in a very ordered manner (the disks stack). The primary reactions of visual transduction occur within the disk membrane. Although electrokinetic techniques (particularly electroorientation) were successfully used for characterizing other cell types, as yet there are no studies investigating, in a noninvasive way, the dielectric permittivity and electric conductivity parameters of the photoreceptor rod that may characterize the functional state of these cells.

After isolation, the ROS in suspension remain viable for a couple of hours (23), representing, thus, a suitable model to study their behavior in AC field. This type of study is pro-

Submitted December 11, 2004, and accepted for publication May 16, 2005.

Address reprint requests to M. Radu, Tel./Fax: 4021-3125955; E-Mail: mradu@ifin.nipne.ro.

0006-3495/05/11/3548/07 $2.00

doi: 10.1529/biophysj.104.057463

mising for developing noninvasive methods such as testing cell viability in retinal transplant and other medical applications. In case of rod-like cells, the electroorientation seems to be the only way to measure the electrical parameters of the cell, because electrorotation and dielectrophoresis are much more appropriate for spherical cells.

In this work we study the orientation behavior of ROS in AC fields of various frequencies. The influence of the cellular electric parameters (such as membrane and cytoplasm conductivity) is revealed and discussed based on an appropriate theoretical model.

MATERIALS AND METHODS

Experimental methods

ROS suspension was prepared by mechanically breaking the connection of ROS to retina (24) as follows.

Frogs *Rana ridibunda* were dark adapted for 24 h and their retinas were isolated from the eye cup and pigment epithelium in aerated Ringer solution (NaCl, 111 mM; KCl, 2.5 mM; $CaCl_2$, 1 mM; $MgCl_2$, 1.6 mM; Hepes, 3 mM; EDTA, 0.01 mM; glucose, 1 mM) buffered to pH 7.7–7.8 with NaOH. A ROS suspension was prepared by a gentle brushing of the retinas into 100 μl solution of 300 mM manitol. To achieve higher values for conductivity of the suspension buffer, small amounts of Ringer solution were added to manitol. Gramicidin A (Fluka, Seelze, Germany) dissolved in ethanol (1 mg/mL) was added to cell suspension to permeabilize the rod membrane.

The measuring chamber consisted of a microscope slide on which a pair of interdigitated electrodes was applied.

A small drop of the cell suspension was deposited between the electrodes. After the cells had settled on the surface of the microscope slide, the AC field was switched on and the orientation of cells was monitored using an image acquisition system.

The AC frequency ranged from 100 Hz to 10 MHz whereas the intensity was adjusted to the minimal value that triggered rod orientation, though not higher than 300 V/cm, a common value in electrokinetic measurements (12,14,15).

Data processing

To establish the turnover frequencies, an image analysis procedure, briefly described below, was used. Two parameters characterizing the orientation of the rods at different frequencies were defined: $L_{\parallel}$ and $L_{\perp}$.

$L_{\parallel}$ is defined as the ratio between the length of cells oriented parallel to the field direction and the total length of cells in the image field. Similarly, $L_{\perp}$ is given by the ratio between the length of cells oriented perpendicular to the field direction and the total length of cells in the same image. To calculate $L_{\parallel}$ and $L_{\perp}$ only the cells oriented at an angle no larger than 15–20° with respect to the chosen direction, were considered. The cells that did not respond to the field action (<10%) were considered adherent to the slide surface and excluded. In suspensions containing a high number of cells, the mutual dielectrophoresis induces cell aggregates formation; only the experiments where the aggregates were very rare have been analyzed (in these cases the cell aggregates have been excluded). $L_{\parallel}$ and $L_{\perp}$ were calculated and plotted versus frequency of the field. The turnover frequency of the cell population was identified as being the cross-point of these two curves (an example is given in Fig. 1). For each field frequency, $L_{\parallel}$ and $L_{\perp}$ were computed using at least five different images. Image analysis was performed by Image Pro Plus software (Silver Spring, MD). Experiments were performed using different values of the external medium conductivity.

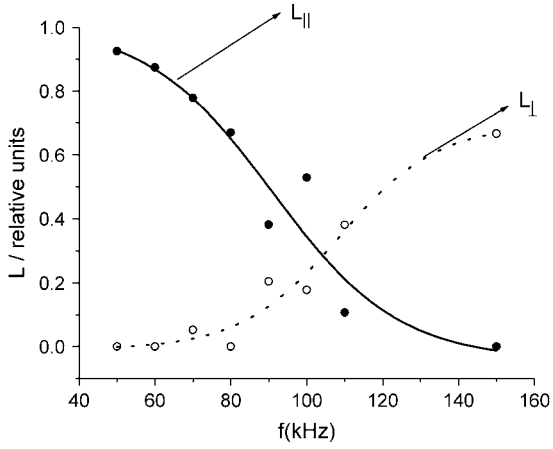

FIGURE 1 Parallel and perpendicular orientation length (L) of the ROS versus frequency of the AC field ($\sigma = 0.015$ S/m).

RESULTS

Theoretical aspects

Interaction of rod-like cells with AC field

To predict the ROS electroorientation a theoretical model of interaction between these cells and AC field was proposed. We assumed that the structure of the rod cell is described by a prolate spheroid with a very long axis. The internal compartment of the ellipsoid is filled with an inhomogeneous medium consisting of alternating layers of membrane and cytoplasm, modeling the photoreceptor disks. A shell covering the ellipsoid models the membrane (Fig. 2).

To build an appropriate model describing the behavior of ROS in external AC field, we followed mainly the work of Kakutani and co-workers (17) and Miller and Jones (12). The electric field components E_{α} can be described in the complex functions formalism as a Fourier series (18,25):

$$\hat{E}_{\alpha} = E_{\alpha}^{m} \sum_{n\geq 1} (a_{\alpha n} - i b_{\alpha n}) \exp(in\omega t) = \sum_{n\geq 1} \hat{E}_{\alpha n}, \qquad (1)$$

where α represents the index for x, y or z axes, E_{α}^{m} are the components of the AC field amplitude using as coordinates

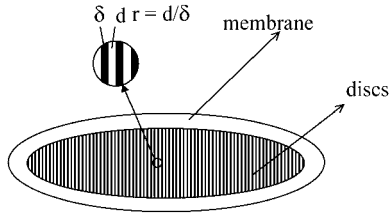

FIGURE 2 Theoretical model of rod photoreceptor cell. The rod photoreceptor cell is approximated using a prolate ellipsoid with a very long axis; the internal compartment of the ellipsoid is filled with an inhomogeneous medium consisting of alternating layers of membrane and cytoplasm as media modeling the disks. A shell covering the ellipsoid modeled the membrane.

the ellipsoid axes, and $a_{\alpha n}$ and $b_{\alpha n}$ are the Fourier coefficients ($\hat{}$ symbolizes the complex form of the parameters).

This field induces, by interfacial polarization, a cellular electric dipole (7) given by:

$$\hat{P}_\alpha = \varepsilon_e \sum_{n\geq 1} \hat{\chi}_{\alpha n}(n\omega)\hat{E}_{\alpha n}, \tag{2}$$

where ε_e is the external solution permittivity and $\hat{\chi}_{\alpha n}$ are the components of the electric susceptibility of the cell. The interaction between the external electric field (evolving only in the xOy plane) and the induced cell dipole leads to an electric torque M_z (25) given by:

$$\langle M_z\rangle = \frac{1}{2}V\varepsilon_e E_x^m E_y^m \sum_{n\geq 1}[(Re\hat{\chi}_{xn} - Re\hat{\chi}_{yn}) \times (a_{xn}a_{yn} + b_{xn}b_{yn}) + (Im\hat{\chi}_{xn} + Im\hat{\chi}_{yn}) \times (a_{yn}b_{xn} - b_{yn}a_{xn})], \tag{3}$$

where V is the cell volume.

In the particular case of an AC field (with no harmonics) in the xOy plane ($a_{x1} = a_{y1} = 1$ and all the other coefficients are 0), the electric torque relation becomes simpler:

$$\langle M_z\rangle = \frac{1}{2}V\varepsilon_e E_x^m E_y^m (Re\hat{\chi}_x - Re\hat{\chi}_y). \tag{4}$$

The electrical susceptibilities are given by the classical solution of the Laplace equation for the ellipsoidal body in external electric field (26):

$$\hat{\chi}_\alpha(\omega) = \frac{\hat{\varepsilon}_\alpha^{ech} - \hat{\varepsilon}_0}{(\hat{\varepsilon}_\alpha^{ech} - \hat{\varepsilon}_0)n_{0\alpha} + \hat{\varepsilon}_0}, \tag{5}$$

where $\hat{\varepsilon}_\alpha^{ech}$ is the equivalent permittivity of a homogeneous ellipsoid electrically equivalent to the cell. The equation for $\hat{\varepsilon}_\alpha^{ech}$ was deduced using an iterative method (11,17):

$$\hat{\varepsilon}_\alpha^{ech} = \hat{\varepsilon}_m \frac{\hat{\varepsilon}_m + (\hat{\varepsilon}_{i\alpha}^{ech} - \hat{\varepsilon}_m)[n_{1\alpha} + \nu(1 - n_{0\alpha})]}{\hat{\varepsilon}_m + (\hat{\varepsilon}_{i\alpha}^{ech} - \hat{\varepsilon}_m)(n_{1\alpha} + \nu n_{0\alpha})}, \tag{6}$$

where $\hat{\varepsilon}_m$ and $\hat{\varepsilon}_{i\alpha}^{ech}$ are the complex forms of the membrane permittivity and the inhomogeneous internal medium, respectively, and $n_{0\alpha}$, $n_{1\alpha}$ are the depolarization coefficients.

Because of the disks stack anisotropy, the $\hat{\varepsilon}_{i\alpha}^{ech}$ values were calculated separately for the directions parallel to the short and long axes of the ellipsoid, respectively:

$$\hat{\varepsilon}_{ia}^{ech} = \frac{\hat{\varepsilon}_d\hat{\varepsilon}_i(r+1)}{\hat{\varepsilon}_i + r\hat{\varepsilon}_d}, \quad \hat{\varepsilon}_{ib}^{ech} = \frac{r\hat{\varepsilon}_i + \hat{\varepsilon}_d}{r+1}, \tag{7}$$

where $\hat{\varepsilon}_d$ is the complex permittivity of the disk, $\hat{\varepsilon}_i$ is the complex permittivity of the cytoplasm, and $r = \delta/l$ is the ratio between the disk thickness and the cytoplasm layer separating two consecutive disks (see Fig. 2).

The cell will be in mechanical equilibrium when one of the ellipsoid axes is parallel with the AC field. The switch between the two possible orientations of the cell (long or short axis parallel with E) occurs when (12):

$$Re\hat{\chi}_x - Re\hat{\chi}_y = 0. \tag{8}$$

Considering the frequency of the AC field as the independent variable, the solutions of this equation represent the turnover frequencies. Because the susceptibilities depend on field frequency and on the electric and geometric parameters of the cell, a change of the orientation will occur when the frequency varies in a large enough range of values. In Table 1 the values of the model parameters are given. Some of the values of the electrical parameters were chosen according to data reported for other cell types because there are no data available for ROS. Particularly, the disk membrane electrical characteristics were assumed to be similar to those of the cell membrane.

Predicted behavior of ROS in AC field

For ROS (geometrically modeled as in Fig. 2), Eq. 8 predicts the shape of the orientation spectrum that defines two areas on the diagram, each of them being characterized by a certain cell orientation (Fig. 3). For lower and higher frequencies, the cells orient parallel to the field; for the intermediate values, the cells orient perpendicular to the field. There is a limiting value of external conductivity up to which electroorientation can be observed.

The lower branch of the spectrum is in the range of 50–500 kHz, much lower than values reported for other types of cells—above 10 MHz (12,14–16). This difference is given by the inhomogenity of the interior compartment of ROS (the presence of the disk stack). Modeling the interior as a homogenous one (made by cytoplasm with usual values for electrical parameters, $\varepsilon_i = 50 \times \varepsilon_0$ and $\sigma_i = 0.5$ S/m), the low branch of the spectrum shifts toward high frequency—above 10 MHz (Fig. 3, *dashed curve*). Several authors tried to describe the orientation of cells in AC fields based on models that use a minimum energy principle. For the cells with a homogenous interior these models predict an additional turnover frequency in the low frequency range (<1 MHz) (13,25). In our case, having a stack-like interior of the cell, the turnover frequency values predicted by the

TABLE 1 Parameters used in the cell model to compute the simulated electroorientation spectra

Parameter	Symbol	Value	Reference
External medium permittivity	ε_e	$80 \times \varepsilon_0$	(12)
External medium conductivity	σ_e	0.007–0.12 S/m	Measured
Membrane permittivity	ε_m	$6 \times \varepsilon_0$	Fitted
Membrane conductivity	σ_m	10^{-7} S/m	(27)
Disk permittivity	ε_d	$6 \times \varepsilon_0$	–
Disk conductivity	σ_d	10^{-7} S/m	–
Cytoplasm permittivity	ε_i	$50 \times \varepsilon_0$	(27,28)
Cytoplasm conductivity	σ_i	0.5 S/m	(29,30)
Vacuum permittivity	ε_0	8.85×10^{-12} F/m	–
Disk thickness/distance between two consecutive disks	r	~1	(31)
Ellipsoid axes ratio	q	~10	Measured
Ellipsoid long axis	a	~25 μm	Measured
Membrane thickness	δ	10 nm	(12)

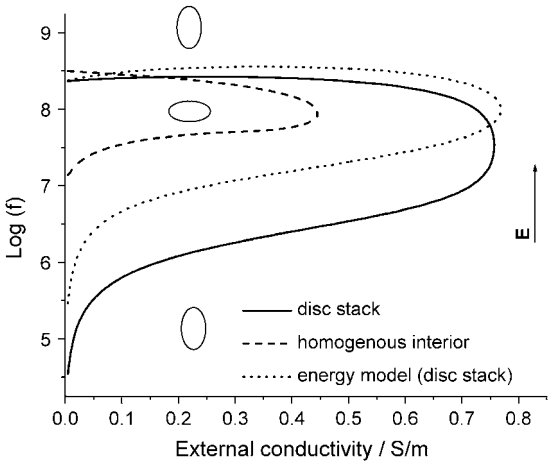

FIGURE 3 Predicted logarithmic representation of the turnover frequency versus external medium conductivity: torque model with disk stack inside the cell (*solid curve*), torque model with a homogenous interior of the cell (*dashed curve*), and the minimum energy model prediction for the cell with a disk stack inside (*dotted curve*).

energy model (Fig. 3, *dotted curve*) are higher than those predicted by the torque model (Fig. 3, *solid curve*).

By varying the electrical parameters of the cell, families of such spectra can be obtained. The particular distribution of disks inside the cell suggests that the cytoplasm conductivity and the distance between two adjacent disks can influence the curve's shape. Fig. 4 shows how these two parameters affect the turnover frequency. The decrease of cytoplasm conductivity restrains the range of external conductivity where the reorientation can be observed (Fig. 4 *a*). The increase of the distance between two consecutive disks enlarges this range. Furthermore, when this distance overcomes twice the thickness of a disk, the upper branch of the spectrum moves to high conductivity values. It becomes, thus, possible, at least theoretically, to induce the reorientation at any value of the external conductivity (Fig. 4 *b*).

An interesting observation emerging from our experiments is the change in the electroorientation spectrum that occurs at different membrane conductivities. In Fig. 5 the turnover frequency was plotted versus external conductivity for three values of the membrane conductivity, within the range of frequency available for our setup. As the graph shows, the turnover frequency rapidly decreases for higher values of the membrane conductivity. Consequently, it can be seen that the spectrum has a limiting value of the external conductivity below which reorientation cannot be observed (Fig. 5, *dotted curve*).

Experimental results

ROS orientation in media of different conductivities

Depending on frequency of the applied AC field, a homogenous population of rod photoreceptor cells orients parallel

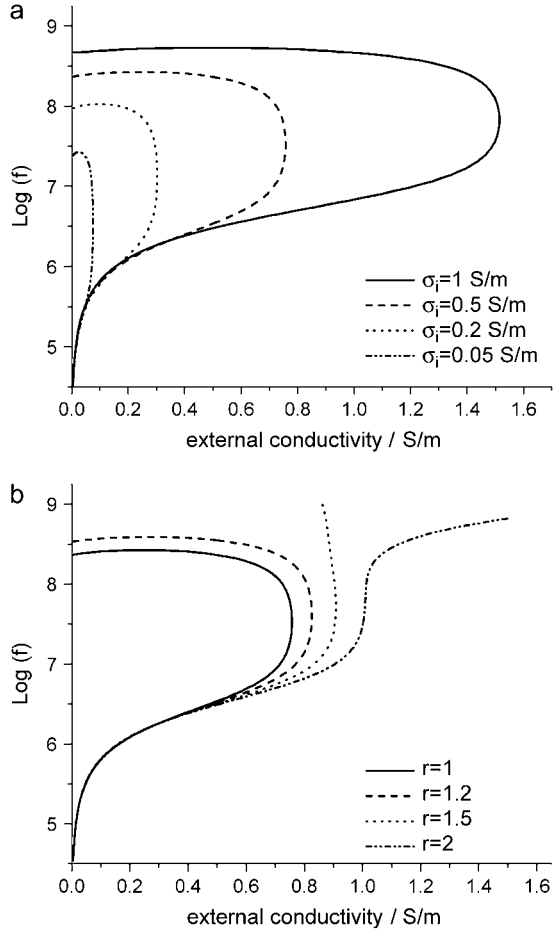

FIGURE 4 Predicted logarithmic representation of the turnover frequency versus external medium conductivity: (*a*) different internal medium conductivities (σ_i); (*b*) different ratios between the thickness of the two successive layers (disk membrane and cytoplasm).

or perpendicular to the field direction (Fig. 6). This behavior was already observed for smaller cells (yeasts, bacteria, erythrocytes, and algae) but not for big cells such as rod photoreceptors.

The frequency at which cells change their orientation from parallel to perpendicular (turnover frequency) depends on the external medium conductivity (13). In our experiments, this turnover frequency ranges between 75 and 500 kHz for cells suspended in buffers having conductivities between 0.007 and 0.09 S/m (Table 2). At higher external conductivity, thermal effects occurred and cells were damaged. The values of turnover frequency found for rods are lower than those reported for other cells (see Table 2 for references) and this is due mainly to the high ROS anisotropy.

The increase of turnover frequency with the external conductivity is in agreement with results reported by other authors for the lower branch of the electroorientation spectrum (9,12). A second turnover frequency for a given conductivity of the suspension solution was reported (12).

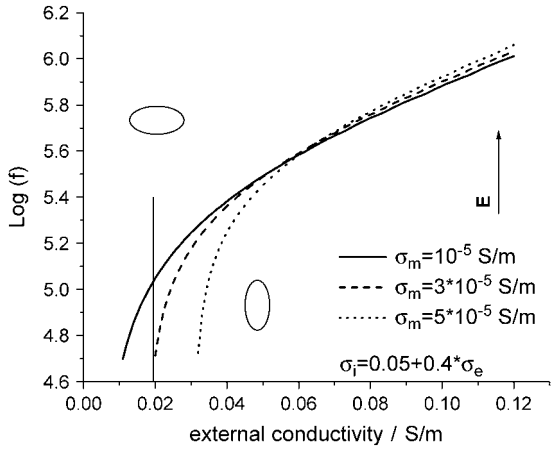

FIGURE 5 Simulation of the change in the electroorientation spectrum of the ROS for different values of membrane conductivity.

This second value is in the high frequency range (>100 MHz) that exceeds the available range of our signal generator (upper limit of the generator was 10 MHz).

Gramicidin-treated ROS

The treatment of ROS suspension with different amounts of gramicidin (final concentration of gramicidin in the suspension was in the range 0–30 μg/mL) results in a drastic change of cell behavior (Table 3). At low gramicidin concentration no change in the turnover frequency was observed. Increasing the concentration, the turnover frequency rapidly decreased to the range of 100–1000 Hz. For the highest gramicidin concentration, the cells aligned only perpendicular to the field, irrespective of frequency.

In a second experiment, cells were treated only with 20 μg/mL gramicidin and the turnover frequency was measured using buffers with conductivities between 0.0013 and 0.12 S/cm. At low conductivity, the turnover frequency decreased to 800 Hz. Increasing the buffer conductivity induced an increase of the turnover frequency with a higher rate than that of control cells (Fig. 7, *solid symbols*).

Data analysis

Using the model to analyze our experiments, the predicted curve fits the experimental data reasonably well (Fig. 7, *open symbols*), indicating that this theoretical approach correctly describes the ROS electroorientation. The measured values are smaller that those predicted by energetic model (Fig. 3, *dotted curve*); thus we may conclude that our model better describes the experimental observations. The parameter values obtained from the fit are given in the Fig. 7 legend.

To observe the influence of internal conductivity of ROS on the turnover frequency, small amounts of gramicidin were added to cell suspensions. The insertion of gramicidin molecules into the lipid bilayer increased the membrane conductivity resulting in an outward flux of ions from the cytoplasm (the ionic concentration in manitol solution was at least two orders of magnitude lower than in the cell interior). In this case we expect a change of the turnover frequency due to: i), the increase of membrane conductivity, and ii), the decrease of cytoplasm conductivity. Changes in the curve shape predicted by the model (Fig. 5) allow us to explain the experimental observations presented in Table 3. Adding gramicidin, the left end of the curve shifts toward right and the turnover frequency at a given external conductivity (0.016 S/m) decreases to the very low frequency range (<1 kHz). A new addition of gramicidin shifts the curve further toward high external conductivity, such that at the same external conductivity, cells may orient only perpendicular to the field. A reorientation is not possible below the limiting value of the external conductivity (Fig. 5, *dotted curve*).

By adding only 20 μg/mL of gramicidin and measuring the turnover frequency for the same range of conductivity as in the experiments without gramicidin, a similar response as above was revealed. The plots of the recorded turnover frequency and the theoretically computed spectrum are presented in Fig. 7 (*solid symbols*; *solid curve*). A shift of the left part of the curve toward higher conductivities is observed. On the other hand, the turnover frequency increases faster for gramicidin-treated cells than for controls. This observation can be explained by the effect of the lower value of the cytosol conductivity (see Fig. 4 *a*). Because not all charged particles in the cell can get out through gramicidin

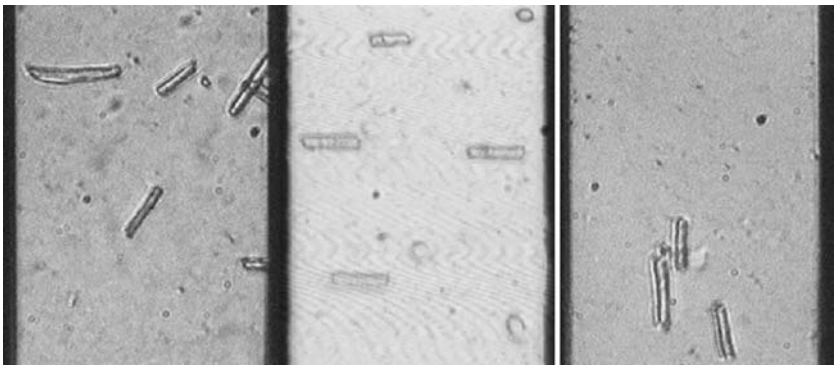

FIGURE 6 An example of various orientation of ROS in AC fields of different frequencies: (*a*) without AC field; (*b*) parallel orientation of the cells (AC, $f =$ 50 kHz; $E \sim 300$ V/cm); (*c*) perpendicular orientation of the cells (AC, $f = 120$ kHz; $E \sim 300$ V/cm).

TABLE 2 Turnover frequency values for different types of cells

Cells/reference	Rods/this article					Yeasts/(9,15)	Erythrocytes/(12)	Algae/(12)
σ_e (S/m)	0.007	0.02	0.025	0.035	0.09	0.001–0.2	0.01–0.25	0.005–0.5
f (MHz)	0.075	0.19	0.25	0.29	0.5	1–200	1–200	1–200

channels, the cytosol conductivity of the treated cells will exceed the external conductivity in the less conductive buffer. For higher buffer conductivity, a linear dependence of cytosol conductivity with respect to that of external buffer may occur (14). Such a dependence was assumed in calculating the curve fitting the data recorded for gramicidin-treated cells (Fig. 7) and the predicted curves in Fig. 5.

DISCUSSION

The predicted values as well as the experimental results presented in the previous section enable us to evaluate some of the ROS electrical properties. The proposed model describes also, in a satisfactory manner, differences observed between electroorientation of rods and other cell types, e.g., yeast or erythrocytes. Thus, reported values of cytosol permittivity of other cells, such as yeast (14) or algae (12), are higher than water permittivity, despite the great content of water in the cell interior. The explanation resides in the fact that cytosol is considered a homogenous medium, electrically equivalent to what is actually a very heterogeneous one. Thus, reported values include contributions of both cytosol and organelles. In addition, such a complex medium has dispersive properties (32). Unlike yeast, erythrocytes have a more homogenous interior (12). In our particular case, the very special disk stack structure of the rods allows a simple modeling of the cell interior electric properties. This results in a more appropriate value for the cytosol permittivity of rods (50 instead of 120 for algae or 85 for yeast). This special internal structure can also explain the smaller values of the turnover frequency compared to other cell types.

The gramicidin channel produces a permeabilization of the plasmalemma for monovalent cations. Distributions of sodium and potassium are the most affected. Because of the low ion concentration in the surrounding medium, monovalent ions tend to flow out of the cell through the gramicidin pores resulting in a decrease of cell cytosol conductivity. The remaining cytosol charge carriers (bivalent and polyvalent ions, etc.) still sustain a minimal value of cytosol conductivity. Adding Ringer solution to increase the conductivity of the external medium, we expect an increase of cytosolic conductivity above the minimal value. This is why a linear increase of cytosol conductivity with that of external medium was assumed in the simulation of the reorientation of gramicidin-treated cells. The best match to the data was obtained for a membrane conductivity of $\sigma_m = 6.5 \times 10^{-5}$ S/m and for the cytosol conductivity of $\sigma_i = 0.045 + 0.4 \times \sigma_e$ S/m. The membrane conductivity increases by almost three orders of magnitude resulting in a 10-fold decrease of the cytosol conductivity. Similar results were reported by Kriegmaier et al., describing reorientation of heated yeast cells (14). The thermal treatment drastically increases the plasmalemma permeability, resulting in a rapid exchange of small ions between the cytosol and the external medium.

To obtain a better fit, a slight increase of the membrane capacity was considered for gramicidin-treated cells ($\varepsilon_m = 7 \times \varepsilon_0$ instead of $\varepsilon_m = 6 \times \varepsilon_0$ for normal cells). There are two reasons for this assumption: i), the inserted gramicidin molecules increase both the membrane permittivity and area, and ii), the water inside gramicidin pores also increases the equivalent membrane permittivity.

TABLE 3 Turnover frequency values for gramicidin-treated cells

Gramicidin (μg/mL)	0	10	20	30
σ_e (S/m)	0.0016	0.0016	0.0016	0.0016
f (kHz)	80	80	<1	Permanent perpendicular orientation

CONCLUSIONS

The electroorientation method proved to be useful for measuring in a noninvasive way the electrical parameters

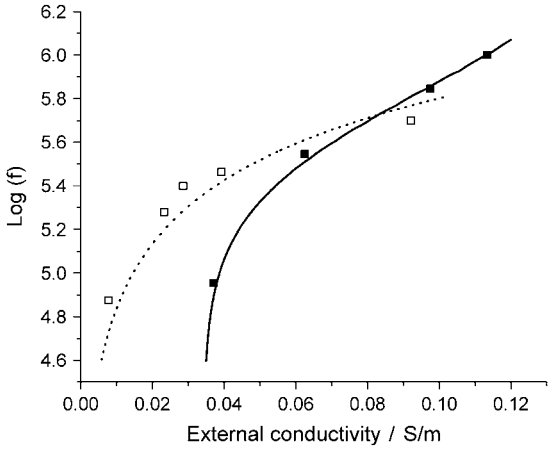

FIGURE 7 The ROS turnover frequency versus external buffer conductivity. For normal cells (*open symbols*) the curve was obtained using the torque model with the parameter values from Table 3, except for the fit parameters: $\varepsilon_m = 6 \times \varepsilon_0$ and $\sigma_i = 0.5$ S/m. For the gramicidin-treated cells (*solid symbols*) the fit curve was obtained with $\sigma_m = 6.5 \times 10^{-5}$ S/m and $\sigma_i = 0.045 + 0.4 \times \sigma_e$ S/m and $\varepsilon_m = 7 \times \varepsilon_0$, the rest of the parameters being as listed in Table 3.

of retinal ROS. The large size and easy-to-model internal structure of the photoreceptor rods are advantages compared to other cells.

The torque theory of electroorientation describes correctly the observed behavior of ROS in an AC field, for the frequency and conductivity ranges available in our experiments. Our theoretical model shows a relationship between the turnover frequency and the internal conductivity. By fitting the experimental data, an evaluation of ROS cytosol conductivity and membrane permittivity was obtained. In addition, a dependence of the orientation spectrum on the ratio between the thickness of the disk and the interdiskal space was demonstrated. Further experiments are necessary to confirm this theoretical prediction.

The change of cytosol ion content due to leakage through the damaged plasmalemma strongly influences the turnover frequency, suggesting that electroorientation can be used as a test for cell membrane integrity and, consequently, for cell viability. It may be considered that the behavior of rod photoreceptor cells in AC fields would thus offer a possibility to evaluate the physiological state of the rod cell via its electrical properties. Determining the shift of the reorientation frequency for a given cell population in a reference external medium may be a first step in the early diagnosis of a cell pathology.

REFERENCES

1. Markx, G. H., and C. L. Davey. 1999. The dielectric properties of biological cells at radiofrequencies: applications in biotechnology. *Enzyme Microb. Technol.* 25:161–171.
2. Pethig, R. 1979. Dielectric and Electronic Properties of Biological Materials. John Wiley & Sons, New York, NY.
3. Gimsa, J. 2001. A comprehensive approach to electro-orientation, electrodeformation, dielectrophoresis and electrorotation of ellipsoid particles and biological cells. *Bioelectrochemistry.* 54:23–31.
4. Jones, T. B. 1995. Electromechanics of Particles. Cambridge University Press, Cambridge, UK.
5. Pohl, H. 1978. Dielectrophoresis. Cambridge University Press, Cambridge, UK.
6. Zimmermman, U. 1996. Electromanipulation of Cells. U. Zimmermman, editor. CRC Press, New York, NY.
7. Turcu, I., and C. M. Lucaciu. 1989. Dielectrophoresis: a spherical shell model. *J. Phys. A: Math. Gen.* 22:985–993.
8. Iglesias, F. J., C. Santamaria, F. J. Asencor, and A. Dominguez. 1996. Dielectrophoresis: effect of nonuniform electrical fields on cell movement. *In* Electrical Manipulation of Cells. P. T. Lynch and M. R. Davey, editors. Chapman & Hall, New York, NY. 71–99.
9. Asencor, F. J., C. Santamaria, F. J. Iglesias, and A. Dominguez. 1993. Dielectric energy of orientation in dead and living cells of *Schizosaccharomyces pombe*. *Biophys. J.* 64:1626–1631.
10. Schwarz, G., M. Saito, and H. Schwan. 1965. On the orientation of nonspherical particles in alternating electrical field. *J. Chem. Phys.* 43:3562–3569.
11. Pauly, H., and H. Schwan. 1966. Dielectric properties and ion mobility in erythrocytes. *Biophys. J.* 6:621–639.
12. Miller, R., and T. Jones. 1993. Electro-orientation of ellipsoidal erythrocytes. Theory and experiment. *Biophys. J.* 64:1588–1595.
13. Saito, M., H. Schwan, and G. Schwartz. 1966. Response of nonspherical biological particles to alternating electric fields. *Biophys. J.* 6:313–327.
14. Kriegmaier, M., M. Zimmermann, K. Wolf, U. Zimmermann, and V. L. Sukhorukov. 2001. Dielectric spectroscopy of *Schizosaccharomyces pombe* using electrorotation and electroorientation. *Biochim. Biophys. Acta.* 1568:135–146.
15. Mischel, M., R. Akermann, R. Hölzel, and I. Lamprecht. 1992. Orientation of elongated cells in AC electromagnetic fields with frequencies up to 150 MHz. *Bioelectrochem. Bioenerg.* 27:413–427.
16. Ignatov, O. V., O. I. Guliya, S. Yu. Shchyogoleva, V. D. Buninb, and V. V. Ignatova. 2002. Effect of p-nitrophenol metabolites on microbial cell electro-optical characteristics. *FEMS Microbiol. Lett.* 214:81–86.
17. Kakutani, T., S. Shibatani, and M. Sugai. 1993. Electrorotation of nonspherical cells: theory for ellipsoidal cells with an arbitrary number of shells. *Bioelectrochem. Bioenerg.* 31:131–145.
18. Turcu, I., and C. M. Lucaciu. 1989. Electrorotation: a spherical shell model. *J. Phys. A: Math. Gen.* 22:995–1003.
19. Haibo, L., and R. Bashir. 2002. Dielectrophoretic separation and manipulation of live and heat-treated cells of Listeria on microfabricated devices with interdigitated electrodes. *Sens. Actuators.* 86:215–221.
20. Yang, J., Y. Huang, X. Wang, X. Wang, F. F. Becker, and P. R. C. Gascoyne. 1999. Dielectric properties of human leukocyte subpopulations determined by electrorotation as a cell separation criterion. *Biophys. J.* 76:3307–3314.
21. Wang, X., F. F. Becker, and P. R. Gascoyne. 2002. Membrane dielectric changes indicate induced apoptosis in HL-60 cells more sensitively than surface phosphatidylserine expression or DNA fragmentation. *Biochim. Biophys. Acta.* 1564:412–420.
22. Marks, G. H., A. Burcak, and A. McGilchrist. 2002. Electro-orientation of Schizosaccharomyces pombe in high conductivity media. *J. Microbiol Methods.* 50:55–62.
23. Baylor, D. A., T. D. Lamb, and K. W. Yau. 1979. The membrane current of single rod outer segments. *J. Physiol.* 288:589–611.
24. Kovacs, E., T. Savopol, and A. Dinu. 1995. The polar behavior of frog photoreceptors. *Biochim. Biophys. Acta.* 1273:217–222.
25. Radu, M. 1999. Effects of variable electric fields on the biological cell suspension. PhD thesis. University of Cluj-Napoca, Romania.
26. Stratton, J. 1941. Electromagnetic Theory. McGraw Hill, New York, NY.
27. Huang, Y., R. Holzel, R. Pethig, and X. B. Wang. 1992. Differences in the AC electrodynamics of viable and non-viable yeast cells determined through combined dielectrophoresis and electrorotation studies. *Phys. Med. Biol.* 37:1499–1517.
28. Raicu, V., G. Raicu, and G. Turcu. 1996. Dielectric properties of yeast cells as simulated by the two-shell model. *Biochim. Biophys. Acta.* 1274:143–148.
29. Holzel, R., and I. Lamprecht. 1992. Dielectric properties of yeast cells as determined by electrorotation. *Biochim. Biophys. Acta.* 1104: 195–200.
30. Chan, K. L., H. Morgan, E. Morgan, I. T. Cameron, and M. R. Thomas. 2000. Measurements of dielectric properties of peripheral blood mononuclear cells and trophoblast cells using AC-electrokinetic techniques. *Biochim. Biophys. Acta.* 1500:313–322.
31. Steinberg, R. H., S. K. Fisher, and D. H. Anderson. 1980. Disc morphogenesis in vertebrate photoreceptors. *J. Comp. Neurol.* 190:501–508.
32. Gimsa, J., T. Muller, T. Schnelle, and G. Fuhr. 1996. Dielectric spectroscopy of single human erytrocytes at physiological ionic strength: dispersion of the cytoplasm. *Biophys. J.* 71:495–506.